

## THE INFLUENCE OF LOW-CONCENTRATION ADDITIVES OF DIMETHYL SULFOXIDE AND FORMAMIDE ON THE STABILITY AND PERFORMANCE OF LITHIUM BIS(TRIFLUOROMETHANESULFONYL)IMIDE-BASED ELECTROLYTE FOR LITHIUM-ION BATTERIES

Amjad Abdelqader<sup>1,\*</sup>, Abdo Mohammed Al-Fakih<sup>1,\*</sup>, Muhammad Amirul Aizat Mohd Abdah<sup>1</sup>, Rawda Maen Sunoqrot<sup>1</sup>, Muhammad Norhaffis Mustafa<sup>2</sup>, Mohamad Hamdi Zainal-Abidin<sup>1</sup>, Ling Shing Liau<sup>1</sup>, Madzlan Aziz<sup>1</sup>

<sup>1</sup>Department of Chemistry, Faculty of Science, Universiti Teknologi Malaysia, 81310 Johor Bahru, Johor, Malaysia

<sup>2</sup>Sunway Centre for Electrochemical Energy and Sustainable Technology (SCEEST), Faculty of Engineering and Technology, Sunway University, No. 5, Jalan Universiti, Bandar Sunway, Subang Jaya, Selangor Darul Ehsan 47500, Malaysia

abedelqader@graduate.utm.my, abdo-pd@utm.my

The development of advanced electrolytes is essential for improving the stability and safety of lithium-ion batteries (LIBs). This study systematically investigated the effect of low concentrations of two polar additives, dimethyl sulfoxide (DMSO) and formamide (FA), in a lithium bis(trifluoromethanesulfonyl)imide (LiTFSI) electrolyte with ethylene carbonate and diethylene carbonate (EC/DEC, 1:1 v/v). Electrolytes containing 2.5 wt% of each additive were prepared and evaluated for ionic conductivity, electrochemical stability window (ESW), Li-ion transference number, and cycling performance in graphite||Li<sup>+</sup> half-cells relative to the blank electrolyte. Ionic conductivity measurements showed that both DMSO and FA reduced conductivity due to higher viscosity and stronger Li<sup>+</sup> solvation. Linear sweep voltammetry (LSV) indicated that while the blank electrolyte exhibited a wide ESW of 5.45 V, the addition of 2.5 wt% DMSO and FA slightly narrowed the window to 5.15 V and 4.98 V, respectively. Both additives increased the Li-ion transference number compared to the blank. Cyclic voltammetry (CV) revealed that DMSO improved interfacial reversibility, whereas FA induced quasi-capacitive behavior with suppressed faradaic processes. However, galvanostatic cycling demonstrated that both additives led to poor coulombic efficiency and unstable cycling, likely due to incompatibility with the graphite anode. Galvanostatic charge-discharge (GCD) results further indicated that low concentrations of DMSO and FA did not enhance long-term cycling stability, probably due to irregular solid electrolyte interphase (SEI) formation, although they may hold potential for high-voltage cathode applications.

**Keywords:** DMSO; formamide; Li-ion batteries; electrochemical tests; LiTFSI-based electrolyte

## ВЛИЈАНИЕ НА МАЛИ КОНЦЕНТРАЦИИ НА АДТИВИТЕ ДИМЕТИЛ СУЛФОКСИД И ФОРМАМИД ВРЗ СТАБИЛНОСТА И ПЕРФОРМАНСИТЕ НА ЕЛЕКТРОЛИТ БАЗИРАН НА ЛИТИУМ БИС(ТРИФЛУОРОМЕТАНСУЛФОНИЛ)ИМИД КАЈ ЛИТИУМ-ЈОНСКИ БАТЕРИИ

Развојот на напредни електролити е од фундаментално значење за подобрувањето на стабилноста и безбедноста на литиум-јонските батерии (LIBs). Во оваа студија систематски е анализиран ефектот од ниски концентрации на два поларни адитива, диметил сулфоксид (DMSO) и формаид (FA), во електролит што е базиран на литиум бис(трифлуорометансулфонил)имид (LiTFSI) со етилен карбонат и диетилен карбонат (EC/DEC, 1:1 v/v). Подготвени беа електролити што содржат по 2.5 % од секој адитив, при што беа евалуирани нивната јонска спроводливост, електрохемискиот потенцијален прозорец на стабилност (ESW), бројот на преносните Li-јони и

циклусната стабилност во графит||Li<sup>+</sup>-полукелиите во споредба со основниот електролит што не содржеше адитиви. Мерењата на јонската спроводливост покажаа дека и DMSO и FA ја намалуваат спроводливоста, пред сè поради зголемениот вискозитет и значително посилената солватација на Li<sup>+</sup>-јоните. Со примена на волтаметрија со линеарна промена на потенцијал (LSV) е покажано дека основниот електролит поседува широк ESW од 5.45 V, додека додавањето на 2.5 % DMSO и FA умерено го намалува прозорецот на 5.15 V и 4.98 V, соодветно. Двата адитива го зголемија преносниот број на Li-јоните во однос на основниот електролит. Цикличната волтаметрија (CV) покажа дека DMSO ја подобрува реверзибилноста, додека FA индуцира квази-капацитетно однесување со намален интензитет на Фарадееви процеси. Сепак, галваностатското циклизирање покажа дека двата адитива доведуваат до ниска електростатска ефикасност и нестабилно циклизирање, најверојатно поради нивната несоодветна компатибилност со графитната анода. Резултатите од галваностатското полнење/празнење (GCD) дополнително укажаа дека ниските концентрации на DMSO и FA не ја подобруваат долгорочната циклусна стабилност, најверојатно поради неправилно формирање на цврстата електролитна интерфазна обвивка (SEI). Овие адитиви сепак, имаат потенцијал за примена во катодни системи што работат на високи напони.

**Клучни зборови:** Диметилсулфоксид; формаид; литиум-јонски батерии; електрохемиски анализи; електролит базиран на литиум бис(трифлуорометансулфонил)имид (LiTFSI)

## 1. INTRODUCTION

For decades, lithium-ion batteries (LIBs), also known as rocking-chair batteries (RCBs), have dominated applications in portable electronics, electric vehicles (EVs), and grid-scale energy storage due to their high energy density and long cycle life.<sup>1-3</sup> Despite this success, the development of electrolyte systems capable of sustaining high power densities while maintaining long-term cycling stability remains a major challenge, particularly under high-voltage operating conditions.

State-of-the-art commercial LIBs employ organic liquid electrolytes consisting of lithium salts dissolved in carbonate-based solvents such as ethylene carbonate (EC), propylene carbonate (PC), dimethyl carbonate (DMC), and diethyl carbonate (DEC). Among lithium salts, lithium hexafluorophosphate (LiPF<sub>6</sub>) is the most widely used; however, it suffers from poor thermal stability and decomposes above 60 °C to form phosphorus pentafluoride (PF<sub>5</sub>) and hydrofluoric acid (HF). These reactive by-products readily attack carbonate solvents and electrode interphases, triggering electrolyte degradation, gas evolution, interfacial instability, and irreversible capacity loss.<sup>4-7</sup> Consequently, conventional carbonate-based electrolytes are increasingly unable to meet the growing demands of high-energy density and high-power LIB applications, thereby motivating the search for advanced electrolyte systems.<sup>1,2,8</sup>

Lithium bis(trifluoromethanesulfonyl)imide (LiTFSI), characterized by its complete dissociation in low dielectric solvents, has been widely regarded as a promising substitute for LiPF<sub>6</sub> due to its enhanced thermal stability, superior electro-

chemical performance, and lower sensitivity to hydrolysis. Moreover, LiTFSI operates within a wide electrochemical window (ESW) (~ 5 V) and offers high solvation ability, which supports high ionic conductivity.<sup>9-12</sup>

Therefore, electrolyte engineering plays a crucial role in developing safer and more advanced LIBs.<sup>8,13-16</sup> In this context, electrolyte enhancers have emerged as a promising approach and have been extensively studied in recent years. When certain additives are used in small amounts (often ≤ 5 vol% or wt%), they can significantly enhance the electrochemical performance and safety of LIBs. Specifically, they play a vital role in improving LIB performance by mitigating electrolyte decomposition, suppressing dendrite formation, and preventing cathode dissolution.<sup>17-21</sup> Furthermore, these additives effectively stabilize the electrolyte, protect both electrodes, expand the ESW, enhance ion conductance, and reduce undesirable side reactions, thereby extending battery life and capacity.<sup>22,23</sup>

A wide range of organic electrolyte additives has been explored, including ionic liquids, small molecules, polymers, fluorinated carbonates, localized high-concentration electrolytes (LHCEs), and organic acids. Fluorinated carbonates and fluorinated co-solvents, for instance, improve oxidative stability and promote the formation of LiF-rich cathode electrolyte interphase (CEI) layers, enabling stable operation at voltages exceeding 4.3 – 4.5 V. However, extensive fluorination often increases cost, raises environmental concerns, and may introduce higher interfacial resistance.<sup>24-26</sup> These limitations highlight the need for alternative additive chemistries that balance stability, conductivity, and sustainability.

Extensive studies have demonstrated the effectiveness of low-concentration additives in stabilizing interphases and enabling fast charging. For instance, Schmidt et al. (2025) showed that 1 wt% organic additives such as tris(trimethylsilyl) phosphite (TMSEPi) and lithium difluoro (oxalate) borate (LiDFOB) significantly enhanced fast-charging capability in graphite/LiNi<sub>0.8</sub>Mn<sub>0.1</sub>Co<sub>0.1</sub>O<sub>2</sub> (NMC811) full cells by forming thin, inorganic-rich solid electrolyte interphase (SEI) and CEI layers.<sup>19</sup> Similarly, Qin et al. (2024) reported that incorporating 4 wt% LiDFOB yielded exceptional capacity retention (94 % after 300 cycles) and reduced polarization due to improved interfacial kinetics as revealed by molecular dynamics simulations.<sup>27</sup>

Parida et al. (2022) further demonstrated that boron-based anion receptor additives suppress ion pairing, enhance Li-ion diffusion, and increase the Li-ion transference number.<sup>28</sup> Notably, Al-Fakih et al. (2025) investigated the role of high-concentration of DMSO and formamide additives through experimental and computational methods. Their key finding was that formamide, a small high-dielectric molecule, nearly doubled the ionic conductivity of a standard LiPF<sub>6</sub> in EC/DMC electrolyte. Furthermore, both additives substantially improved anodic stability, raising the decomposition potential from 3.42 V in the baseline electrolyte to 5.43 V (formamide) and 4.40 V (DMSO) versus Li/Li<sup>+</sup>.<sup>18</sup>

Formamide is a highly polar aprotic solvent with an exceptionally high dielectric constant (~ 111 at 25 °C), enabling efficient lithium-salt dissociation and reduced ion pairing in electrolyte systems. Its strong donor ability and hydrogen-bonding capability allow formamide to actively influence Li<sup>+</sup> solvation structures and interfacial chemistry when introduced at low concentrations. During initial cycling, formamide can preferentially decompose, forming nitrogen- and oxygen-containing species that contribute to a compact, ionically conductive SEI, thereby suppressing continuous electrolyte degradation and reducing polarization. In addition, its high boiling point (210 °C), low vapor pressure, and thermal stability enhance electrolyte safety under high-rate or elevated-temperature conditions.<sup>29</sup>

On the other hand, dimethyl sulfoxide (DMSO), although not widely adopted in commercial LIBs, exhibits distinct physicochemical advantages that warrant systematic investigation. DMSO is a polar aprotic solvent with a high dielectric constant (46.46), a strong donor number, and an exceptional ability to solvate lithium salts, which facilitates enhanced salt dissociation and

modified solvation structures. In addition, DMSO exhibits a relatively wide electrochemical stability window, a high boiling point, and low vapor pressure, contributing to improved thermal safety. Importantly, its strong coordinating ability enables DMSO to directly participate in interphase chemistry, potentially regulating the composition and stability of the SEI.<sup>22,30</sup>

To date, the SEI formation and electrochemical stability in DMSO-modified and formamide-modified LiTFSI-based electrolytes have not been comprehensively investigated, especially under low additive concentrations relevant to practical electrolyte formulations. This study examines the implementation of DMSO and formamide as potential electrolyte additives aimed at improving the electrochemical stability window and the electrochemical redox behavior of LIB half-cells. Each additive was individually mixed at a concentration of 2.5 wt% in the blank electrolyte (1 M LiTFSI in EC/DEC 1:1, (v/v)). Key electrolyte characteristics, including ionic conductivity, electrochemical stability, Li-ion transference number and cyclic performance were systematically evaluated. A comprehensive set of techniques, including ionic conductivity measurements, linear sweep voltammetry (LSV), galvanostatic charge-discharge (GCD) testing and cyclic voltammetry (CV) was utilized to thoroughly investigate the performance and stability of the electrolytes.

## 2. EXPERIMENTAL

### 2.1. Materials and chemicals

Lithium bis[trifluoromethanesulfonyl]imide (LiTFSI (99.9 %)), ethylene carbonate (EC (98 %)), diethyl carbonate (DEC (99 %)), formamide (99 %), and dimethyl sulfoxide (DMSO (99%)) were obtained from Merck, stored in an argon-filled glove box and were utilized without further purification. The LiTFSI salt was dried in an oven overnight at 60 °C. Polyvinylidene fluoride (PVDF (99.5 %)), *N*-methyl-2-pyrrolidone (NMP (99 %)), super P and graphite were obtained from Sigma Aldrich, USA and utilized as received. Celgard® polypropylene membranes and current collector substrates (copper foil) were purchased from Merck, Germany and KGC Resources Sdn. Bhd., Malaysia.

### 2.2. Preparation of electrolyte samples and graphite electrode

The electrolyte samples were prepared by mixing 2.5 wt% of each additive into the blank

electrolyte hereafter referred to as 2.5 wt% DMSO and 2.5 wt% FA. The blank electrolyte was prepared by dissolving 1.0 mol/l LiTFSI salt in (EC/DEC 1:1, v/v). These formulation guarantees consistency in the electrolyte composition, enabling reliable and reproducible electrochemical measurements.

For the slurry preparation, the binder solution was prepared by dissolving 1 g PVDF in 10 ml NMP and stirred for 24 h at room temperature. Subsequently, graphite (85 wt%) and super P (5 wt%) were ground and mixed with the binder (10 wt%). Then, the resulting mixture was sonicated and stirred for an additional 24 h to ensure complete homogenization. Lastly, the slurry was doctor-bladed onto a copper foil current collector utilizing an electrode automatic coating machine, yielding a thickness of approximately 200  $\mu\text{m}$ . After drying overnight at 70  $^{\circ}\text{C}$ , the resulting film was punched into 16 mm diameter discs (area of 2  $\text{cm}^2$ ), and further dried in an oven at 80  $^{\circ}\text{C}$  for 2–3 h to eliminate residual moisture before transfer to the glove-box, yielding an active mass loading of  $\sim 2\text{--}3 \text{ mg/cm}^2$ . Each cell was assembled using approximately 60  $\mu\text{l}$  of electrolyte to ensure complete wetting of the separator and electrodes and to provide stable cycling performances and reliable electrochemical data.

### 2.3. Characterization

The fabrication of CR2032 coin cells was carried out in an argon glove-box ( $\text{O}_2$ ,  $\text{H}_2\text{O}$  content  $< 0.01 \text{ ppm}$ ) utilizing the Li||Li and graphite||Li<sup>+</sup> half-cell as depicted in Figure 1. Ionic conductivities were measured at room temperature using the EUTECH PC2700 conductivity meter, Thermo Scientific<sup>TM</sup>, USA. The instrument was first calibrated with a standard potassium chloride solution before measurement, each sample was measured three times and the average value was calculated.

Linear sweep voltammetry (LSV) tests were carried out at room temperature using an Autolab Potentiostat (PGSTAT 30), China, scans were conducted at a rate of 0.01 V/s over a voltage range of 0 V – 6 V to assess the stability of each electrolyte. Li-ion transference number ( $t_{\text{Li}^+}$ ) was determined using the chronoamperometry technique, performed on the Versa STAT 4A under a constant potential of 1 V. Electrochemical impedance spectroscopy (EIS) measurements were carried out before and after chronoamperometric polarization over a frequency range from 1 MHz to 0.1 Hz with an amplitude of 5 mV. All measurements were performed using a Gamry Interface 1010E potentiostat.

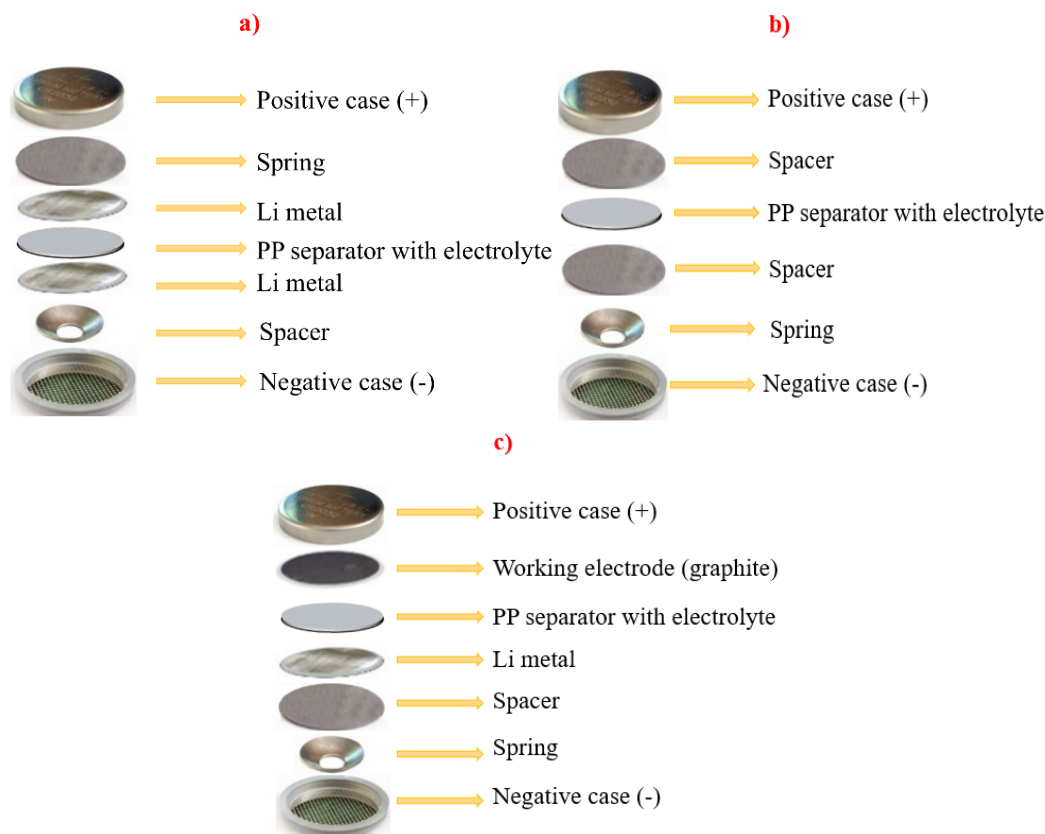


**Fig. 1.** CR2032 schematic assembly used for (a) EIS and chronoamperometry, (b) LSV, and (c) CV and GCD

Cyclic voltammetry (CV) tests were performed using an Autolab Potentiostat (PGSTAT 30), China. The scans were applied over a potential range of 0.01 V – 2 V at a scan rate of 0.2 mV/s for 3 cycles to obtain detailed electrochemical responses and reversibility. Notably, the graphite electrode was subjected to drying at 70 °C for 2 h to ensure complete removal of ambient moisture.

Galvanostatic charge-discharge (GCD) cyclic discharge behavior of the half-cell was evaluated at a current density of 0.1 A/g. The tests were conducted within a potential range (0.01V – 2V) versus Graphite|Li<sup>+</sup> employing a Neware battery tester (CT-4008Tn – 5V10 mA), China. Prior to testing, the assembled cells were rested overnight to ensure adequate electrode wettability.

### 3. RESULTS AND DISCUSSION

#### 3.1. Ionic conductivity

The ionic conductivity of each electrolyte was measured at room temperature, as summarized in Table 1. Ionic conductivity is a critical parameter governing battery electrochemical performance, as it reflects the ease of ion transport through the electrolyte and strongly influences both energy efficiency and power capability.<sup>31</sup> In this study, the conductivities of the blank electrolyte and electrolytes containing 2.5 wt% DMSO or 2.5 wt% FA were evaluated.

Table 1

*Ionic conductivity of the studied electrolytes measured at room temperature*

Sample	Ionic conductivity (mS/cm) at room temperature
Blank electrolyte	7.46
2.5 wt% DMSO	6.83
2.5 wt% FA	6.17

The blank electrolyte exhibited the highest conductivity (7.46 mS/cm). Upon the addition of either additive, a slight decrease in conductivity was observed. Specifically, the electrolyte containing 2.5 wt% DMSO showed a conductivity of 6.83 mS/cm, while that containing 2.5 wt% FA exhibited the lowest value of 6.17 mS/cm. This reduction was primarily attributed to the higher viscosities of DMSO and formamide relative to the blank electrolyte; even at low concentrations, their incorporation increased the overall electrolyte viscosity, thereby hindering Li<sup>+</sup> mobility.

In addition, both additives possess strong solvation abilities and can strongly coordinate with lithium ions, leading to the formation of more stable solvation shells and a reduced population of free charge carriers, which further contributes to the observed decrease in ionic conductivity.

#### 3.2. Linear sweep voltammetry

Linear sweep voltammetry (LSV) is a widely used electrochemical technique for determining electrolyte decomposition thresholds and evaluating the electrochemical stability window (ESW), which defines the safe operating voltage range of electrochemical systems. In this study, LSV was employed to examine the influence of formamide and DMSO additives on the ESW of the electrolytes (Fig. 2).

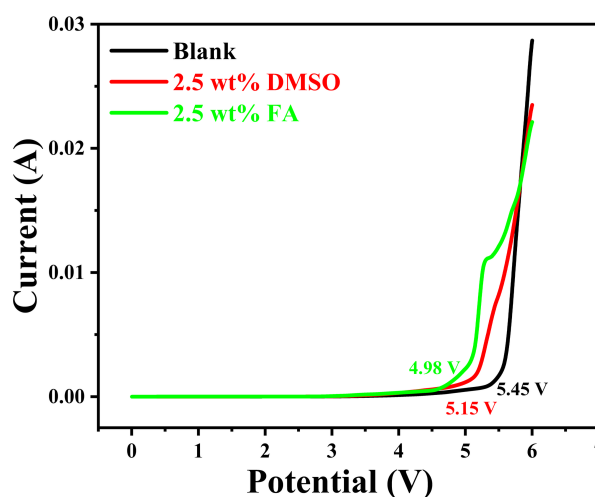


Fig. 2. LSV profiles of the studied electrolyte systems measured at room temperature at a scan rate of 0.01 V/s

For the blank electrolyte, stable behavior was observed up to 5.45 V. Beyond this potential, a sharp rise in current occurred, indicating the onset of oxidative decomposition of the electrolyte. This abrupt increase in current corresponded to electron loss and confirmed electrolyte oxidation at high potentials. Notably, conventional LiPF<sub>6</sub>-based carbonate electrolytes typically exhibited oxidative decomposition at significantly lower voltages, generally around 4.3 V, highlighting the enhanced anodic stability of the LiTFSI-based system investigated in this work.<sup>18,32,33</sup>

In contrast, LiTFSI-based electrolytes operate over a higher voltage range (above 5 V), underscoring their superior thermal stability and wider ESW compared with conventional LiPF<sub>6</sub>-based electrolytes. Upon the incorporation of additives, a

slight reduction in the ESW and a less stable current response were observed. For the electrolyte containing 2.5 wt% DMSO, the current remained stable up to 5.15 V, beyond which a noticeable increase in current signalled the onset of electrolyte decomposition.

Nevertheless, when compared with the typical LiPF<sub>6</sub>-based electrolytes, which decomposed at approximately 4.3 V, the LiTFSI-based systems investigated here still exhibited a substantially broader operating voltage window, highlighting a marked improvement in electrochemical stability.<sup>18,34</sup> Accordingly, the incorporation of low concentrations of DMSO did not extend the ESW. Similarly, the electrolyte containing 2.5 wt% formamide exhibited a slightly reduced voltage stability limit of 4.98 V.

Overall, the addition of low concentrations of DMSO or formamide to the LiTFSI-based electrolyte did not broaden the ESW, as the blank electrolyte already possessed a wide stability window of 5.45 V. These LSV results emphasized the intrinsic capability of LiTFSI-based electrolytes to delay electrolyte decomposition, thereby enabling more stable and safer operation at elevated voltages compared with conventional LiPF<sub>6</sub>-based electrolytes.

From a practical perspective, a wider ESW was directly correlated with higher achievable energy density and improved battery safety.<sup>35</sup> Highly stable electrolytes helped minimize the risks of unintended side reactions, gas generation, and electrode breakdown. These findings indicated that incorporation of LiTFSI salt could enable high-voltage batteries, thereby promoting fast-charging applications.

### 3.3. Lithium-ion transference number ( $t_{Li^+}$ )

The lithium-ion transference number ( $t_{Li^+}$ ) is a critical parameter governing concentration polarization and, consequently, the rate capability and cycling stability of lithium-ion batteries. A higher  $t_{Li^+}$  indicates that a larger fraction of the ionic current is carried by Li<sup>+</sup> ions, which promotes a more uniform salt concentration during operation and enables higher power densities. In this study, the  $t_{Li^+}$  was calculated using equation 1, with the interfacial resistances determined from electrochemical impedance spectroscopy (EIS) measurements, as shown in Figure S1, where  $t_+$  denotes the Li-ion transference number,  $I_s$ : steady-state current,  $I_0$ : the initial current,  $\Delta V$ : the applied potential difference,  $R_0$  and  $R_s$ : the bulk resistances before and after polarization, respectively.

For all electrolyte formulations, the Nyquist plots exhibited only minor variations in the semi-circle diameter after polarization, indicating that the interfacial resistance remained largely stable throughout the measurement. This behavior suggested that no significant interfacial degradation occurred under the applied experimental conditions, thereby supporting the reliability of the steady-state current method employed for  $t_{Li^+}$  determination. Moreover, the low solution resistance ( $R_s$ ) combined with a well-defined Warburg diffusion tail reflected high ionic conductivity of the investigated electrolytes, which was consistent with the conductivity values summarized in Table 1. Notably, the absence of a pronounced increase in impedance after polarization implied that the electrolyte–electrode interfaces remained kinetically stable throughout the experiment.

$$t_+ = \frac{I_s(\Delta V - I_0 R_0)}{I_0(\Delta V - I_s R_s)} \quad (1)$$

As shown in Table 2, the blank electrolyte, serving as the baseline, exhibited a  $t_{Li^+}$  number of 0.35. This value was consistent with, albeit slightly higher than, the widely cited literature benchmark of approximately 0.27 for standard carbonate-based electrolytes.<sup>36,37</sup> The incorporation of 2.5 wt% DMSO led to a substantial increase in the lithium-ion transference number, reaching a value of 0.45. This enhancement highlighted the strong coordination between DMSO and Li<sup>+</sup> ions, which effectively shielded the cation and weakened its interaction with the TFSI anion. Notably, DMSO possessed a high donor number, and its strong Lewis basicity enables more effective coordination with Li<sup>+</sup> ions. As a result, DMSO was likely to enter the primary solvation shell, forming a larger and more stable solvation complex that promoted preferential Li<sup>+</sup> transport.

Table 2

*Lithium-ion transference number ( $t_{Li^+}$ ) of the studied electrolytes determined at room temperature utilizing a constant potential of 1 V*

Sample	$I_0$ (mA)	$I_s$ (mA)	$t_{Li^+}$
blank	4.51	2.92	0.35
2.5 wt% DMSO	0.49	0.27	0.45
2.5 wt% FA	0.21	0.13	0.38

In contrast, the electrolyte containing 2.5 wt% formamide exhibited a more modest transference number of 0.38, representing only a slight

improvement over the blank electrolyte. This behavior was attributed to the smaller molecular size and different molecular geometry of formamide compared with DMSO, which could influence ion-solvent interactions and the relative mobilities of charge carriers. Overall, the transference number results confirmed that the strategic use of strongly solvating additives was an effective approach for modulating ion transport in electrolytes. Among the additives studied, DMSO proved particularly effective, whereas formamide provided a moderate enhancement, underscoring the importance of molecular-level electrolyte design in controlling lithium-ion transport.

### 3.4. Cyclic voltammetry

Cyclic voltammetry (CV) was employed to evaluate the redox behavior, interfacial stability, and reversibility of the Graphite||Li<sup>+</sup> half-cells containing the studied electrolytes over a potential range of 0.01 – 2.0 V at a scan rate of 0.2 mV/s for three consecutive cycles (Fig. 3). CV analysis provided valuable mechanistic insight into lithium intercalation/deintercalation kinetics, SEI formation, and polarization effects at the electrode-electrolyte interface.

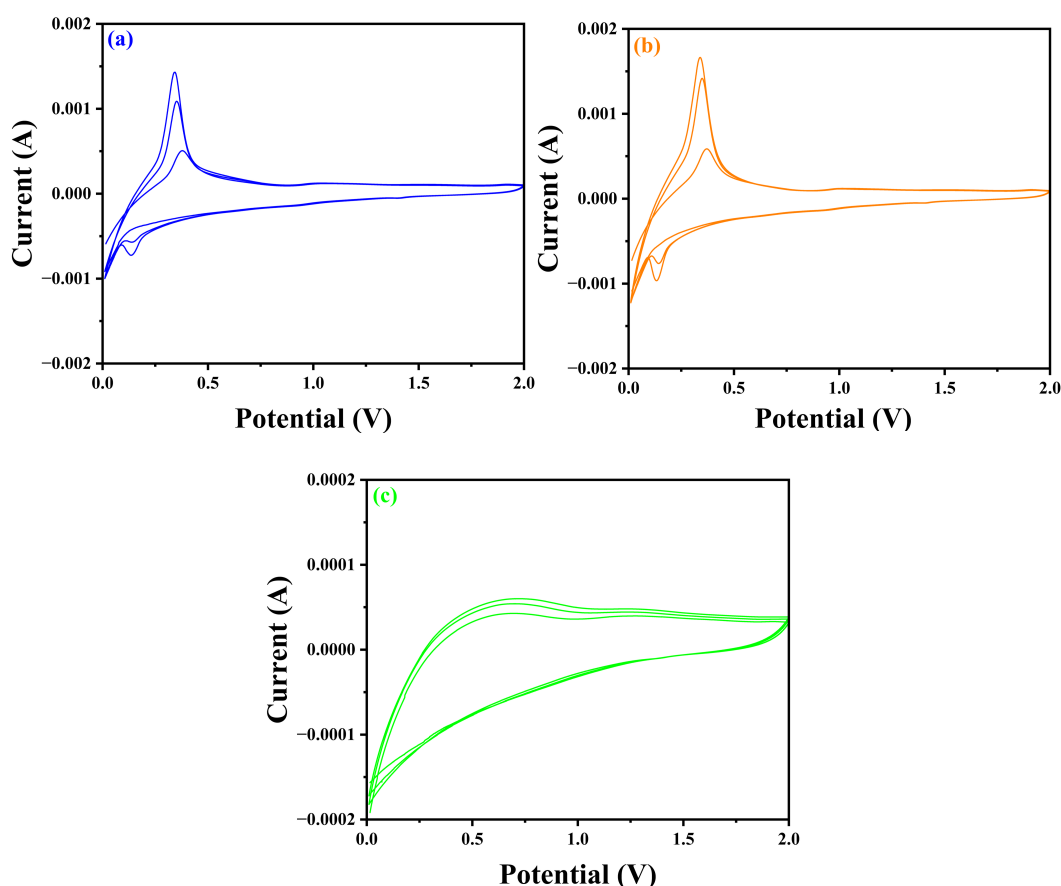


**Fig. 3.** Cyclic voltammograms of graphite||Li<sup>+</sup> half-cell at a scan rate of 0.2 mV/s for 3 cycles at room temperature for a) blank electrolyte, b) 2.5 wt% DMSO, and c) 2.5 wt% FA

As shown in Figure 3(a), the blank LiTFSI-based electrolyte exhibited a pronounced cathodic peak around approximately 0.5 V during the first scan, which is commonly attributed to electrolyte reduction and the initial formation of the SEI on the graphite surface. This irreversible process was a characteristic of SEI nucleation and growth, during which electrolyte components decompose to form a passivating layer. In subsequent cycles, the cathodic feature diminished markedly and the CV

curves became highly reproducible, with nearly overlapping anodic and cathodic branches. This behavior indicated that the SEI formed during the first cycle was sufficiently compact and electronically insulating to suppress further electrolyte decomposition.

The appearance of reversible anodic and cathodic peaks in the range of 0.2 – 0.3 V corresponded to the staging transitions associated with lithium intercalation and deintercalation in graph-

ite. The reduced peak separation and increased symmetry observed in later cycles suggested decreased polarization and improved kinetic reversibility of the  $\text{Li}^+$  insertion/extraction processes.<sup>33</sup>

Upon incorporation of 2.5 wt% DMSO (Fig. 3(b)), the CV profiles exhibited enhanced overlap between successive cycles compared with the blank electrolyte, indicating improved interfacial stability and more consistent electrochemical behavior. The reduced potential separation between anodic and cathodic peaks reflected lower charge-transfer resistance and diminished polarization, implying that DMSO favorably modified the solvation environment and SEI chemistry. In addition, the higher current response observed throughout the voltage window suggested enhanced charge-storage capability and improved utilization of active material. These features indicate that DMSO promoted more efficient  $\text{Li}^+$  transport across the electrode electrolyte interface, consistent with its strong solvating ability and high donor number. Accordingly, the redox features indicated that the presence of DMSO extended the accessible electrochemical window relative to the blank electrolyte, in good agreement with the LSV results.

In contrast, the CV response of the electrolyte containing 2.5 wt% formamide (Fig. 3(c)) displayed a markedly different behavior, characterized by a quasi-rectangular shape with the absence of distinct redox peaks. Such a profile was indicative of rapid and highly reversible surface-controlled charge storage rather than diffusion-limited faradaic intercalation processes. This behavior implied that formamide altered the interfacial chemistry

and solvation structure in a manner that disfavored bulk graphite intercalation while promoting capacitive charge storage. The nearly linear current–potential relationship further supported a dominant electric double layer capacitance mechanism, where current scaled proportionally with scan rate.<sup>38,39</sup>

Mechanistically, Li-ions did not intercalate deeply into the bulk crystal structure, instead, they were rapidly and reversibly adsorbed onto the surface of the graphite. Due to a fast current response, the rate of ion adsorption/desorption changed linearly, resulting in a nearly constant current, and hence the rectangular CV profile. Although CV measurements were conducted at a single scan rate in this study, the observed differences in peak definition, symmetry, and current response provide clear mechanistic insight. In particular, the sharp peaks observed in the blank and DMSO-containing electrolytes were consistent with diffusion-controlled intercalation processes, whereas the quasi-rectangular response observed for the formamide-containing electrolyte was characteristic of a surface-controlled kinetics. Table 3 summarizes the CV metrics and mechanistic interpretations of the studied samples.

Overall, the CV results demonstrated that electrolyte additives strongly influence the interfacial electrochemical mechanism. DMSO enhanced intercalation reversibility and reduced polarization, whereas formamide suppressed faradaic processes and shifted charge storage toward a capacitive regime, highlighting the critical role of molecular-level electrolyte design in regulating electrode kinetics.

Table 3

*Cyclic voltammetry (CV) metrics and interpretations of the studied samples*

Sample	Anodic peak current	SEI band (0.5 – 0.9 V)	Peak separation	Interpretation
Blank	1 – 1.2 mA	Clear in the 1 <sup>st</sup> cycle (0.5 – 0.6 V)	0.15 – 0.18 V	low polarization, high reversibility
2.5 wt% DMSO	1.3 – 1.5 mA	Clear, slightly reshaped (additive-modified SEI) (0.45 – 0.55 V)	0.08 – 0.12 V (smaller than blank)	low polarization, high reversibility
2.5 wt% FA	Not observed	Quasi-capacitive behavior	Not observed	high polarization, no reversibility

### 3.5. Galvanostatic charge-discharge cycling

The cycling stability of the cells was evaluated to assess the performance of the LiTFSI-based blank electrolyte in comparison with electrolytes containing DMSO or formamide additives. Cycling tests were conducted for 50 cycles within a poten-

tial window of 0.01 – 2.0 V versus  $\text{Li}/\text{Li}^+$  in graphite|| $\text{Li}^+$  half-cells at a current density of 0.1 A/g. As shown in Figure 4, the LiTFSI-based blank electrolyte exhibited good interfacial stability, as evidenced by a high coulombic efficiency (CE) of 99.77 % maintained throughout cycling. This behavior indicated the formation of a robust and sta-

ble SEI during the initial cycles, which effectively suppressed continuous electrolyte decomposition and enabled sustained  $\text{Li}^+$  transport.

In contrast, the incorporation of DMSO or formamide as additives led to pronounced deterioration in cell performance. The electrolyte containing 2.5 wt% formamide exhibited a reduced CE of approximately 78.9 %, indicating significant loss of intercalated  $\text{Li}^+$  within the graphite anode. This behavior suggested uncontrolled electrolyte decomposition and the formation of an unstable SEI. Notably, the CE gradually increased during subsequent cycles, implying partial stabilization of the interphase over time.

The electrolyte containing 2.5 wt% DMSO displayed even poorer performance, with an initial CE of approximately 21 %, followed by an increase to over 90 % by the tenth cycle and a subsequent decline to about 34 % after 20 cycles. This irregular CE evolution deviated from the typical behavior observed during SEI formation, where an initial efficiency loss was generally followed by stabilization. The observed trend indicated that DMSO underwent continuous reductive decomposition on the graphite surface rather than forming a protective SEI layer, highlighting its high reactivity toward the graphite anode.

Generally, a decrease in CE during the first few cycles was expected due to SEI formation; however, the persistent instability observed here confirmed the incompatibility of DMSO with graphite-based anodes under the investigated conditions.<sup>40,41</sup>

Overall, these results demonstrated that both DMSO and formamide were incompatible with graphite anode under the studied conditions. In contrast, the LiTFSI-based electrolyte maintained a very high CE of approximately 99.7 %.

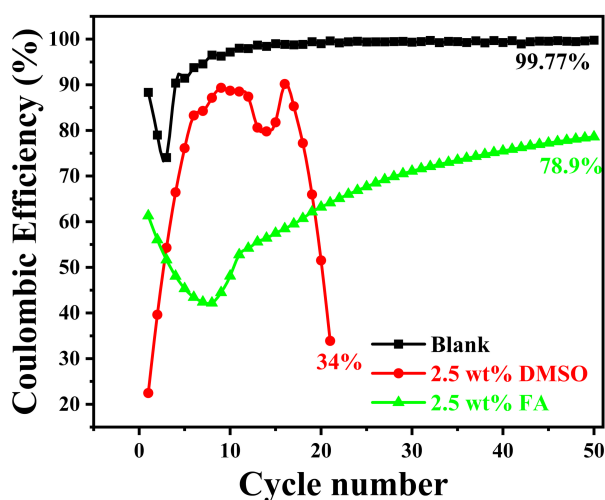


Fig. 4. Coulombic efficiencies of graphite|| $\text{Li}^+$  half-cell for the studied electrolyte systems

#### 4. CONCLUSION

This work provided a systematic and quantitative assessment of the effects of low concentrations (2.5 wt%) of polar additives, namely DMSO and formamide, on the physicochemical and electrochemical behavior of a LiTFSI-based carbonate electrolyte in graphite|| $\text{Li}^+$  half-cells. Both additives exhibited strong solvating ability toward  $\text{Li}^+$  ions, leading to a moderate decrease in ionic conductivity relative to the blank electrolyte, consistent with increased viscosity and reinforced solvation shells. Despite this reduction, the lithium-ion transference number was enhanced from 0.35 for the blank electrolyte to 0.45 and 0.38 for DMSO- and FA-containing electrolytes, respectively, demonstrating the effectiveness of polar additives in modulating ion-transport properties.

Electrochemical stability analysis revealed that the pristine LiTFSI-based electrolyte possessed a wide anodic stability window of 5.45 V, while the addition of DMSO and FA resulted in slightly reduced stability limits of 5.15 V and 4.98 V, respectively. Cyclic voltammetry provided mechanistic insight, showing that DMSO improved interfacial reversibility and reduced polarization during  $\text{Li}^+$  intercalation/deintercalation, whereas formamide suppresses diffusion-controlled faradaic processes and promoted a predominantly surface-controlled, capacitive charge-storage mechanism.

However, galvanostatic cycling clearly demonstrated that neither DMSO nor formamide was compatible with graphite anodes under the investigated conditions. Both additives led to poor coulombic efficiencies and unstable cycling trend which were attributed to irregular and non-protective SEI formation. In contrast, the blank LiTFSI-based electrolyte maintained excellent interfacial stability, achieving a high coulombic efficiency of 99.77 %, confirming its strong compatibility with graphite.

While incompatible with graphite, the high anodic stability of over 5 V of the DMSO and formamide-containing electrolytes highlighted their potential suitability for high-voltage cathode systems. Future work will focus on evaluating these electrolytes in full cells employing high-voltage cathodes such as NMC811, performing detailed interfacial surface analyses, including X-ray photoelectron spectroscopy (XPS), scanning electron microscopy (SEM), and conducting scan-rate-dependent CV studies to further elucidate charge-storage mechanisms. Overall, this study provided fundamental guidance for redirecting po-

lar solvent additives toward next-generation high-voltage LIBs chemistries.

**Acknowledgments.** The authors would like to acknowledge the financial support from the Ministry of Higher Education (Malaysia) under the Fundamental Research Grant Scheme (FRGS) (FRGS/1/2024/TK08/UTM/02/19) and Universiti Teknologi Malaysia (UTM) for supporting this research under the Geran Penyelidikan Hi-Tech (F4).

[Cost center no.: Q.J130000.4654.00Q23, Registration no.: UTM.(S).J.09.01/25.11/3 F4(2.).]

## REFERENCES

- (1) Deshmukh, K.; Varade, K.; Rajesh, S.; Sharma, V.; Kabudake, P.; Nehe, S.; Lokawar, V. Sodium-ion batteries: state-of-the-art technologies and future prospects. *Journal of Materials Science* **2025**, *60* (8), 3609–3633. <https://doi.org/10.1007/s10853-025-10671-6>
- (2) Yang, J.; Wang, Y.; Liu, Y.; Duan, G.; Liang, Z.; Han, J.; Huang, Y.; Han, X.; Zhang, C.; He, S. Design of cyclic carbonate-based electrolytes for HC anodes towards improved low-temperature performance in lithium-ion batteries system. *Fuel* **2025**, *379*, 133048. <https://doi.org/10.1016/j.fuel.2024.133048>
- (3) Gulaboski, R. The future of voltammetry. *Macedonian Journal of Chemistry and Chemical Engineering* **2022**, *41* (2), 1–12. <https://doi.org/10.20450/mjccce.2022.2555>
- (4) Wang, Z.; Hofmann, A.; Hanemann, T. Low-flammable electrolytes with fluoroethylene carbonate based solvent mixtures and lithium bis(trifluoromethanesulfonyl) imide for lithium-ion batteries. *Electrochimica Acta* **2019**, *298*, 960–972. <https://doi.org/10.1016/j.electacta.2018.12.117>
- (5) Alhadj, M.; Liau, L. S.; Al-Fakih, A. M. Polymer electrolytes for sustainable energy: A minireview on zero-carbon storage and conversion. *ACS Applied Polymer Materials* **2025**, *7* (6), 3442–3465. <https://doi.org/10.1021/acsapm.4c03958>
- (6) Senthil, C.; Subramani, A.; Gupta, R. K.; Sofer, Z. Functional electrolyte additives: A pinch of salt/solvent to an electrolyte for high energy density lithium-ion and lithium–metal batteries. *Small* **2025**, 2504276. <https://doi.org/10.1002/smll.202504276>
- (7) Terreblanche, J. S.; Luo, T.; Piper, L. F.; Dose, W. M. Degradation pathways in lithium-ion batteries with ethylene carbonate-free electrolytes. *Advanced Energy Materials* **2025**, 2404427. <https://doi.org/10.1002/aenm.202404427>
- (8) Li, J.; Fan, Z.; Guo, J.; Zheng, J.; Xie, W.; Fang, Z.; Yan, C.; Wang, R.; Chen, H.; He, H. Insights into the efficient roles of boron-containing additives for Li-ion batteries. *Surfaces and Interfaces* **2024**, 104309. <https://doi.org/10.1016/j.surfin.2024.104309>
- (9) Yang, Y.-P.; Huang, A.-C.; Tang, Y.; Liu, Y.-C.; Wu, Z.-H.; Zhou, H.-L.; Li, Z.-P.; Shu, C.-M.; Jiang, J.-C.; Xing, Z.-X. Thermal stability analysis of lithium-ion battery electrolytes based on lithium bis(trifluoromethanesulfonyl) imide-lithium difluoro (oxalato) borate dual-salt. *Polymers* **2021**, *13* (5), 707. <https://doi.org/10.3390/polym13050707>
- (10) Kim, Y.; Moysiadou, A.; Egorov, K.; Rentsch, D.; Battaglia, C. A Strategy to prevent fluorine-induced transition metal dissolution in lithium-ion batteries. *Advanced Energy and Sustainability Research* **2025**, 2500194. <https://doi.org/10.1002/aesr.202500194>
- (11) Teoh, K. S.; Melchiorre, M.; Darlami Magar, S.; Leibing, C.; Ruffo, F.; Gómez-Urbano, J. L.; Balducci, A. formulation and recycling of a novel electrolyte based on bio-derived  $\gamma$ -valerolactone and lithium bis(trifluoromethanesulfonyl) imide for lithium-ion batteries. *Small* **2025**, *21* (9), 2407850. <https://doi.org/10.1002/smll.202407850>
- (12) Lai, Z.; You, D.; Wei, W.; Xiong, H. Conformation-assisted solid-solid phase transition of LiTFSI electrolyte salt and the lithium ion coordination. *Giant* **2024**, *20*, 100330. <https://doi.org/10.1016/j.giant.2024.100330>
- (13) Li, L.; Liu, J.; Li, L.; Chen, J.; Liu, J.; Zhou, R.; Zhang, L. Pentafluorophenyl diethoxy phosphate: An electrolyte additive for high-voltage cathodes of lithium-ion batteries. *Journal of Energy Storage* **2024**, *87*, 111364. <https://doi.org/10.1016/j.est.2024.111364>
- (14) Song, C.; Han, S. H.; Moon, H.; Choi, N. S. Unlocking fast-charging capabilities of lithium-ion batteries through liquid electrolyte engineering. *EcoMat* **2024**, *6* (7), e12476. <https://doi.org/10.1002/eom2.12476>
- (15) Dai, S.; Fang, W.; Wang, T.; Gao, Y.; Zhang, T.; Qin, Z.; Chen, G.; Zhou, X. Progresses on advanced electrolytes engineering for high-voltage lithium metal batteries. *Chemical Engineering Journal* **2024**, *500*, 157269. <https://doi.org/10.1016/j.cej.2024.157269>
- (16) Tomich, A. W.; Chen, J.; Carta, V.; Guo, J.; Lavallo, V. Electrolyte engineering with carboranes for next-generation Mg batteries. *ACS Central Science* **2024**, *10* (2), 264–271. <https://doi.org/10.1021/acscentsci.3c01176>
- (17) Bolloju, S.; Vangapally, N.; Elias, Y.; Luski, S.; Wu, N.-L.; Aurbach, D. Electrolyte additives for Li-ion batteries: classification by elements. *Progress in Materials Science* **2024**, 101349. <https://doi.org/10.1016/j.pmatsci.2024.101349>
- (18) Al-Fakih, A. M.; Tan, J.; Aziz, M.; Abdah, M. A. A. M.; Maarof, H.; Mamat, C. R.; Zainal-Abidin, M. H.; Matmin, J. Effect of formamide and DMSO additives on the electrolyte properties of a lithium-ion battery: Experimental and theoretical study. *Electrochimica Acta* **2025**, *525*, 146095. <https://doi.org/10.1016/j.electacta.2025.146095>
- (19) Schmidt, R.; Liu, C.; Cui, Z.; Manthiram, A. Unveiling the influences of electrolyte additives on the fast-charging performance of lithium-ion batteries. *Journal of Power Sources* **2025**, *627*, 235844. <https://doi.org/10.1016/j.jpowsour.2024.235844>
- (20) Tesatchabut, P.; Muangkasem, P.; Kuananusont, N.; Limthongkul, P.; Eiamlamai, P. Enhancing the performance of LiNi<sub>0.8</sub>Mn<sub>0.1</sub>Co<sub>0.1</sub>O<sub>2</sub>-based pouch cells through advanced electrolyte additive systems for high-temperature lithium-ion batteries. *Journal of Power Sources* **2024**, *623*, 235470. <https://doi.org/10.1016/j.jpowsour.2024.235470>
- (21) Alhadj, M.; Attan, N.; Abedelqader, A.; Aziz, M. Suppressing dendritic growth in lithium metal batteries: Re-

- cent strategies, mechanistic, and technological advances. *Journal of Power Sources* **2025**, *660*, 238520. <https://doi.org/10.1016/j.jpowsour.2025.238520>
- (22) Kang, G.; Zhong, G.; Cai, K.; Ma, J.; Biao, J.; Cao, Y.; Lu, S.; Yu, K.; Kang, F.; Cao, Y. Dimethyl sulfide electrolyte additive enabled high-voltage lithium-ion battery. *ACS Energy Letters* **2024**, *9* (6), 2572–2581. <https://doi.org/10.1021/acsenergylett.4c00519>
- (23) Gulaboski, R.; Mirceski, V.; Lovric, M. Critical aspects in exploring time analysis for the voltammetric estimation of kinetic parameters of surface electrode mechanisms coupled with chemical reactions. *Macedonian Journal of Chemistry and Chemical Engineering* **2021**, *40* (1), 1–9.
- (24) Xia, L.; Lee, S.; Jiang, Y.; Xia, Y.; Chen, G. Z.; Liu, Z. Fluorinated electrolytes for Li-ion batteries: the lithium difluoro (oxalato) borate additive for stabilizing the solid electrolyte interphase. *ACS Omega* **2017**, *2* (12), 8741–8750. <https://doi.org/10.20450/mjcc.2021.2270>
- (25) Li, Z.; Chen, Y.; Yun, X.; Gao, P.; Zheng, C.; Xiao, P. Critical review of fluorinated electrolytes for high-performance lithium metal batteries. *Advanced Functional Materials* **2023**, *33* (32), 2300502. <https://doi.org/10.1002/adfm.202300502>
- (26) Efaw, C. M.; Wu, Q.; Gao, N.; Zhang, Y.; Zhu, H.; Gering, K.; Hurley, M. F.; Xiong, H.; Hu, E.; Cao, X. Localized high-concentration electrolytes get more localized through micelle-like structures. *Nature Materials* **2023**, *22* (12), 1531–1539. <https://doi.org/10.1038/s41563-023-01700-3>
- (27) Qin, G.; Zhang, J.; Chen, H.; Li, H.; Hu, J.; Chen, Q.; Hou, G.; Tang, Y. Lithium difluoro (oxalato) borate as electrolyte additive to form uniform, stable and LiF-rich solid electrolyte interphase for high performance lithium ion batteries. *Surfaces and Interfaces* **2024**, *48*, 104297. <https://doi.org/10.1016/j.surfin.2024.104297>
- (28) Parida, R.; Pahari, S.; Jana, M. Introducing the potency of new boron-based heterocyclic anion receptor additives to regulate the solvation and transport properties of Li-ions in ethylene carbonate electrolyte of Li-Ion battery: An atomistic molecular dynamics study. *Journal of Power Sources* **2022**, *521*, 230962. <https://doi.org/10.1016/j.jpowsour.2021.230962>
- (29) Yang, H.; Qi, Y.; Wang, Z.; Pan, Q.; Zhang, C.; Yan, J.; Cen, K.; Bo, Z.; Ostrikov, K. Sodium nitrate/formamide deep eutectic solvent as flame-retardant and anticorrosive electrolyte enabling 2.6 V safe supercapacitors with long cyclic stability. *Energy & Environmental Materials* **2024**, *7* (3), e12641. <https://doi.org/10.1002/eem2.12641>
- (30) Kao-ian, W.; Nguyen, M. T.; Yonezawa, T.; Pornprasertsuk, R.; Qin, J.; Sivamogsatham, S.; Kheawhom, S. Highly stable rechargeable zinc-ion battery using dimethyl sulfoxide electrolyte. *Materials Today Energy* **2021**, *21*, 100738. <https://doi.org/10.1016/j.mtener.2021.100738>
- (31) Zhang, G.; Deng, X.; Li, J.; Wang, J.; Shi, G.; Yang, Y.; Chang, J.; Yu, K.; Chi, S.-S.; Wang, H. A bifunctional fluorinated ether co-solvent for dendrite-free and long-term lithium metal batteries. *Nano Energy* **2022**, *95*, 107014. <https://doi.org/10.1016/j.nanoen.2022.107014>
- (32) Jiang, B.; Li, H.; Luo, B.; Liu, L.; Chu, L.; Zhang, Q.; Li, M. Vinyltrimethylsilane as a novel electrolyte additive for improving interfacial stability of Li-rich cathode working in high voltage. *Chinese Chemical Letters* **2024**, *35* (2), 108649. <https://doi.org/10.1016/j.cclet.2023.108649>
- (33) Li, L.; Liu, M.; Yang, P.; Yuan, W.; Chen, J. Tris (pentafluoro) phenylborane electrolyte additive regulates the highly stable and uniform CEI membrane components to improve the high-voltage behaviors of NCM811 lithium-ion batteries. *Journal of Colloid and Interface Science* **2024**, *676*, 613–625. <https://doi.org/10.1016/j.jcis.2024.07.155>
- (34) Zarei-Jelyani, M.; Salehi, A.; Maghsoudi, R.; Babaiee, M.; Masoomi, M.; Ganji, M. J. Z. Design and electrochemical assessment of a LiPF<sub>6</sub>-based electrolyte with dopamine and LiDFOB additives for high-rate lithium-ion batteries. *Electrochimica Acta* **2025**, 147008. <https://doi.org/10.1016/j.electacta.2025.147008>
- (35) Li, J.; Fan, Z.; Ye, H.; Zheng, J.; Qiu, J.; He, H.; Liu, P.; He, M.; Liu, H.; Hoa, N. D. Novel sulfur-based electrolyte additive for constructing high-quality sulfur-containing electrode-electrolyte interphase films in sodium-ion batteries. *Chemical Engineering Journal* **2024**, *489*, 151188. <https://doi.org/10.1016/j.cej.2024.151188>
- (36) Peng, J.; Meng, J.; Wu, J.; Deng, Z.; Lin, M.; Mao, S.; Stroe, D.-I. A comprehensive overview and comparison of parameter benchmark methods for lithium-ion battery application. *Journal of Energy Storage* **2023**, *71*, 108197. <https://doi.org/10.1016/j.est.2023.108197>
- (37) Woo, S.-G.; Hwang, E.-K.; Kang, H.-K.; Lee, H.; Lee, J.-N.; Kim, H.-s.; Jeong, G.; Yoo, D.-J.; Lee, J.; Kim, S. High transference number enabled by sulfated zirconia superacid for lithium metal batteries with carbonate electrolytes. *Energy & Environmental Science* **2021**, *14* (3), 1420–1428. <https://doi.org/10.1039/D0EE03967E>
- (38) Azmi, S.; Koudahi, M. F.; Frackowiak, E. Reline deep eutectic solvent as a green electrolyte for electrochemical energy storage applications. *Energy & Environmental Science* **2022**, *15* (3), 1156–1171. <https://doi.org/10.1039/D1EE02920G>
- (39) Lokhande, A.; Kanagaraj, A.; Managutti, P. B.; Kaewmaraya, T.; Hussain, T.; Choi, D. Experimental and theoretical investigation of silicon-based carbon composite electrode for high performance Li-ion capacitors. *Journal of Alloys and Compounds* **2024**, *1003*, 175665. <https://doi.org/10.1016/j.jallcom.2024.175665>
- (40) Qin, M.; Zeng, Z.; Wu, Q.; Yan, H.; Liu, M.; Wu, Y.; Zhang, H.; Lei, S.; Cheng, S.; Xie, J. Dipole–dipole interactions for inhibiting solvent co-intercalation into a graphite anode to extend the horizon of electrolyte design. *Energy & Environmental Science* **2023**, *16* (2), 546–556. <https://doi.org/10.1039/D2EE03626F>
- (41) Wang, F.; Wang, J.; Li, G.; Guo, Z.; Chu, J.; Ai, X.; Song, Z. A high-energy dual-ion battery based on chloride-inserted polyviologen cathode and LiCl/DMSO electrolyte. *Energy Storage Materials* **2022**, *50*, 658–667. <https://doi.org/10.1016/j.ensm.2022.05.055>